MODELLING OF THE MULTIPHASE BEHAVIOR OF METHANE–ETHANE–NITROGEN MIXTURE AT LOW TEMPERATURES WITH AN EQUATION OF STATE

Roumiana P. STATEVA and Stefan G. TSVETKOV

Institute of Chemical Engineering,
Bulgarian Academy of Sciences, acad. G. Bontchev str., bl. 103, Sofia 1113, Bulgaria

Received June 12, 1991
Accepted September 23, 1991

The paper discusses modelling of the multiphase behavior of methane–ethane–nitrogen mixture, which is of a considerable interest for the natural gas and oil industries. The thermodynamic model is a modified Redlich–Kwong–Soave equation of state. The computer algorithm is based on a new approach to solving the isothermal multiphase flash problem, when the number and identity of the phases present at equilibrium are unknown in advance. The results demonstrate that the Redlich–Kwong–Soave equation of state and the algorithm applied predict with reasonable accuracy the complicated phase behavior and the region of L_1L_2V equilibrium, observed in the experiment, of the methane–ethane–nitrogen system.

The design and operation of low temperature processes, petroleum reservoir management, enhanced oil recovery and separation processes in the oil and gas industry involve modelling phase behavior of multicomponent hydrocarbon mixtures with inorganic gases. Special attention is paid to acquiring a knowledge of methane–ethane–nitrogen mixture's phase behavior and an ability to predict and model it since these components will generally account for 95% of the total material processed. Nitrogen has been also known to induce liquid–liquid–vapor (LLV) behavior in liquefied natural gas (LNG) systems and the presence of a third phase can often cause problems in natural gas industry.

The paper addresses the computerized prediction of the methane–ethane–nitrogen equilibrium multiphase behavior at low temperatures with a new algorithm. It uses a modified "classical" equation of state – the Redlich–Kwong–Soave (RKS EOS) (ref.[9]), applied to both phases (liquid and vapor).

The Topography of the Multiphase Behavior

There is only a limited number of binary systems exhibiting LLV behavior related to natural gas processing and nitrogen–ethane is among the most prominent ones.

A schematic diagram of the *P–T* projection of the LLV space for a ternary system with no constituent binary LLV behavior present[1,2] is shown in Fig. 1. For such system,

the three-phase region is bounded from above by a K-point locus (L–L=V), from below by a LCST locus (L=L–V) and at low temperatures by a Q-point locus (S–L–L–V). These three loci intersect at invariant points for the ternary system: the K-point and LCST loci – at a tricritical point t (L=L=V), while the Q-point locus terminates at points (S–L–L=V) and (S–L=L–V) from above and below, respectively.

If one of the constituent binary pairs in the multicomponent system is LLV immiscible, the LLV region (Fig. 1) will be changed since a truncation of the phase space is introduced (Fig. 2). For a system for which the third species (methane in our case) is miscible with both members of the immiscible pair, the resulting phase space should be as the shaded part, shown in Fig. 2.

However, the binary immiscible pair (C_2H_6–N_2) that truncates the LLV space differs in end points from the case, shown in Fig. 2. It would span the LLV space from a position on the LCST locus to a position on the Q-point locus (Fig. 3). Methane has an additional role to created a three-phase L_1L_2V surface in thermodynamic phase space, extending from the binary L_1L_2V locus upward in temperature. This trend occurs because methane is of intermediate volatility when compared to the components of the constituent immiscible binary mixture.

A schematic diagram of the P–T projection of the LLV space for the CH_4–C_2H_6–N_2 mixture is shown in Fig. 4.

Thermodynamic Model

A modified RKS EOS (refs[4 - 6]) is chosen for the thermodynamic model. The temperature relation for α was taken after Soave[9].

$$\alpha(T_r) = [1 + K(1 - T_r^{0.5})]^2 \tag{1}$$

However K was assumed to be related to temperature[4 - 6]

$$K = K_0 + [K_1 + K_2(K_3 - T_r^{0.5})](1 + T_r^{0.5})(0.7 - T_r) \tag{2}$$

and K_0 – a generalized function of the accentric factor. The coefficients K_1, K_2 and K_3 are charasteristic for a given compound and are determined from saturated vapor pressure data[6].

The mixing rules used are the "classical" one-fluid van der Waals:

$$a_m = \sum\sum x_i x_j a_{ij}\,, \qquad b_m = \sum x_i b_i \tag{3}$$

$$a_{ij} = (1 - k_{ij})\,(a_{ii}\,a_{jj}) \qquad (i \neq j)\,. \tag{3a}$$

The binary interaction parameters k_{ij} are assumed to be a linear function of temperature[5]:

$$k_{ij} = k'_{ij} + k^{(T)}_{ij} (T - 273.15), \quad (4)$$

while k'_{ij} and $k^{(T)}_{ij}$ are obtained by processing VLE data accesible from many sources for the respective constituent binary pair[6]. The usual concept is that interaction parameters, obtained from an entirely different type of phase behavior, would not predict correctly a multiphase behavior. Hence, one of the goals of the present investigation is to analyse

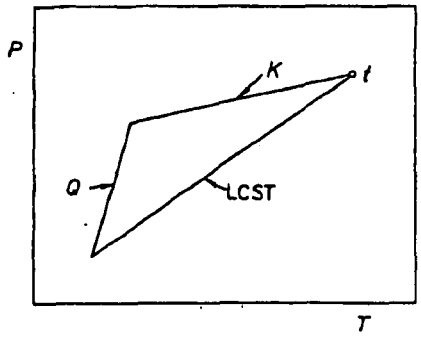

FIG. 1
A schematic diagram of the pressure–temperature projection of the LLV space for a ternary system with no constituent binary LLV behavior present

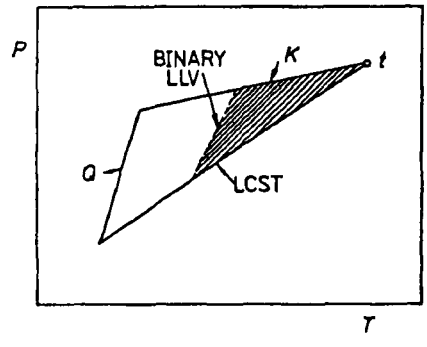

FIG. 2
A binary LLV locus superimposed on the LLV space. The shaded area depicts expected LLV behavior of a mixture with a third component miscible with both components in the immiscible pair

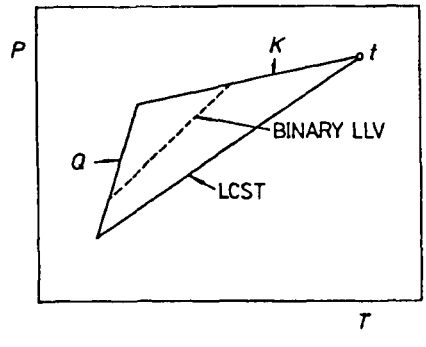

FIG. 3
The LLV locus of N_2–C_2H_6 superimposed on the LLV space

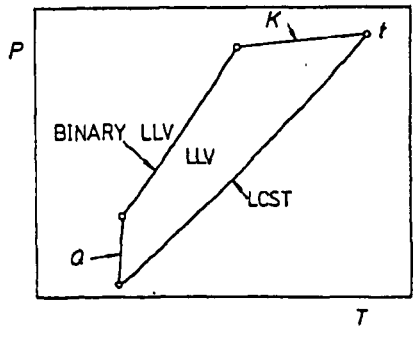

FIG. 4
A schematic diagram of the P–T projection of the LLV space for the CH_4–C_2H_6–N_2 mixture

how well the modified RKS EOS, with the mixing rules and interaction parameters applied, will predict the region of the experimentally observed L_1L_2V behavior.

Computer Algorithm

The computer algorithm for modelling the phase behavior of the methane–ethane–nitrogen mixture is based on a new approach to solving the isothermal multiphase flash problem, when the number and identity of the phases present at equilibrium are unknown in advance. Two interlinked problems have to be solved by this method: firstly the phase configuration with the minimum Gibbs energy has to be identified and secondly the compositions of the equilibrium phases at the specified temperature and pressure have to be calculated. These tasks are realized through:

– a rigorous method for thermodynamic stability analysis, based on the well known tangent-plane criterion[11,12], and applied as a first step[7];

– an efficient short-cut procedure for the final phase identification and equilibrium calculations, applied as a second.

The primary role of the thermodynamic stability analysis is to determine whether the mixture is stable or unstable and in the latter case to provide a geometric information about the molar Gibbs energy hypersurface (g surface). The information will give an idea about how g is folded. If it is quite "pleated", this indicates a possible existence of different types of phase equilibria – "vapor–liquid", "liquid–liquid", "liquid–liguid–vapor", etc., of which only one is stable (the one with minimum Gibbs energy). The geometric information, however, has to acquire a mathematical form in order to be successfully interpreted and used further on. A mathematical formalization of the above problem has been suggested in the form of the so-called "stationary criterion"[10]. A different mathematical formalization is given in the form of a new functional[7]:

$$\Phi(\underset{\sim}{y}) = \sum_{i=1}^{N_c} (k_{i+1}(y) - k_i(y))^2 , \tag{5}$$

where

$$k_i(y) = \ln \varphi_i(y) + \ln y_i - h_i \quad i = 1,2,...,N_c , \tag{5a}$$

$$h_i = \ln z_i + \ln \varphi_i(z) \qquad i = 1,2...,N_c , \tag{5b}$$

$$k^{(y)}_{N_c+1} = k_1(y) .$$

The functional $\Phi(y)$ is positive, its zeroes are its minima and coincide with the solutions (stationary points) of the stationary criterion[10].

The key point of the stability analysis, in the sense of the above ideas, rests on finding all (the maximum possible number of) zeroes y^s of the functional $\Phi(y)$. Such information can be related directly to g and interpreted further on because the zeroes (y^s) of the functional $\Phi(y)$ correspond to points on the g hypersurface, where the local tangent hyperplane is parallel to that at z. To each y^s a number k^s corresponds, such that:

$$k^s = \ln y_i^s + \ln \varphi_i(y^s) - h_i \quad i = 1, 2, ..., N_c \ .$$

Geometrically k^s is the vertical distance in Gibbs free energy between such two hyperplanes.

The method chosen for solution of the corresponding mathematical problem, Eqs (*5a*) – (*5b*), is the quasi-Newton Broyden–Fletcher–Goldfarb–Shanno (BFGS) with a line search[8].

When multiple zeroes of $\Phi(y)$ are found this speaks of a quite "pleated" g surface. Furthermore, y^s "phase identification", either "liquid" or "vapor" (in terms of molar Gibbs energy), gives an insight into the anticipated phase behavior of the system. Thus the rigorous stability analysis[7] provides means to solve the multiphase flash problem in a new way avoiding the alternative application of stability analysis and a phase-splitting technique, each consecutive time on a higher level, as will be demonstrated further on.

The zeroes of $\Phi(y)$ provide also a set of good initial composition estimates for the expected equilibrium calculations. If, however, zeroes of the functional $\Phi(y)$ are not found, that does not guarantee that the system is stable, which is one of the primary limitations of the tangent-plane stability analysis. In such cases an additional alternative procedure is provided, which helps to distinguish metastable from stable mixtures[7].

When stability analysis has been successfully completed the following information is available:

– positive or positive and negative or negative numbers k^s;

– zeroes of the functional – y^s.

Once initial composition estimates, y^s, have been generated by the thermodynamic stability analysis, liquid–vapor and liquid–liquid flash calculations are performed. They put the final touch to forming the picture of the phase behavior of the system and provide the equilibrium compositions.

The general algorithm applied consists of the following steps:

1. Form two groups of zeroes of the functional – a group of zeroes with a "liquid" identification (y_L^s) and a group of those (usually one) with a "vapor" identification – y_V^s. The feed, depending on its identification, is included in one of the groups as well.

2. Provide different sets of initial estimates for the K values:

– for the vapor–liquid flash algorithm $K_i = y_{iV}^s / y_{iL}^s$;

– for the liquid–liquid flash algorithm $K_i = y^s_{iL_2}/y^s_{iL_1}$, where $y^s_{L_2}$ is a "liquid" zero with a larger volume than $y^s_{L_1}$;

It is recommended to combine zeroes with positive and negative k^s, if such are available.

3. Select the one set of K-values, leading to composition estimates with lower Gibbs energy, for the liquid–liquid and the liquid–vapor flash calculations[11].

4. Perform liquid–liquid and liquid–vapor flash calculations.

5. Discard from further consideration a flash calculation if it has converged to a phase split outside the physical limits $0 < \alpha < 1$, required by the Rachford–Rice formula. The phase identification and the equilibrium calculations of the system at the specified temperature and pressure are completed.

Otherwise continue with step 6.

6. Calculate the Gibbs energy of the projection of the feed on the tangent plane to g surface at the equilibrium concentrations: $G_{Feed} = G_V\alpha + G_L(1 - \alpha)$, where G_V is the molar Gibbs energy of the vapor phase in the case of a liquid–vapor calculations or the molar Gibbs energy of the lighter liquid phase in the case of the liquid–liquid flash calculations.

7. If $\Delta G_{Feed}^{(L-L)-(L-V)} < -5 \cdot 10^{-4}$ the system is identified as a liquid–liquid. If $\Delta G_{Feed}^{(L-V)-(L-L)} < -5 \cdot 10^{-4}$ the system is identified as a liquid–vapor. The value $5 \cdot 10^{-4}$ is found empirically to be a sufficient upper bound.

If $\text{abs}[\Delta G_{Feed}^{(L-L)-(L-V)}] \leq 5 \cdot 10^{-4}$, continue with step 8.

8. Perform a liquid–vapor flash calculation if the liquid–liquid solution has a lower Gibbs energy. Flash the liquid phase with the lower Gibbs energy (let it be L_1). Otherwise perform the corresponding flash calculations for the phase with the lower Gibbs energy in the liquid–vapor system. If this is the liquid phase, liquid–liquid calculations are run. Both flash calculations require initial estimates. They can be selected, according to step 3. Continue with step 9. If the corresponding flash calculations converge with a phase split outside the physically acceptable bounds $0 < \beta < 1$, the system is classified either as a liquid–liquid or as a liquid–vapor, depending on the result obtained in step 7.

9. Calculate either

i) $G_{Feed}^{L-L-V} = \alpha G_{L2} + (1 - \alpha)[\beta G_{V'} + (1 - \beta)G_{L'}] = \alpha G_{L2} + (1 - \alpha)G_{Feed}^{L'-V'}$ or

ii) $G_{Feed}^{L-L-V} = \alpha G_V + (1 - \alpha)[\beta G_{L''} + (1 - \beta)G_{L'}] = \alpha G_V + (1 - \alpha)G_{Feed}^{L'-L''}$.

Continue with step 10.

10. If either $G_{Feed}^{L-L-V} \leq G_{Feed}^{L-L}$ (case *i*) or $G_{Feed}^{L-L-V} \leq G_{Feed}^{L-V}$ (case *ii*), the system is identified as a liquid–liquid–vapor. The corresponding equilibrium compositions are either $x_{L'}$, x_{L2}, $y_{V'}$ (case *i*) or $x_{L'}$, $x_{L''}$, y_V (case *ii*).

The algorithm is demonstrated on four simplified paradigms, which summarize most of the cases encountered when solving the isothermal multiphase flash problem.

The example of a thermodynamically more stable liquid–liquid equilibrium is used only to elucidate the ideas.

CASE *A*
STABILITY ANALYSIS
LL

Conclusion: L_1L_2

CASE *B*
STABILITY ANALYSIS
LL LV

$\Delta G_{\text{Feed}}^{(L-L)-(L-V)} < -5 \cdot 10^{-4}$

Conclusion: L_1L_2

CASE *C*
STABILITY ANALYSIS
LL LV

$\text{abs}[\Delta G_{\text{Feed}}^{(L-L)-(L-V)}] \leq 5 \cdot 10^{-4}$

LV – fails

Conclusion: L_1L_2

CASE *D*
STABILITY ANALYSIS
LL LV

$\text{abs}[\Delta G_{\text{Feed}}^{(L-L)-(L-V)}] \leq 5 \cdot 10^{-4}$

LV

$G_{\text{Feed}}^{LLV} \leq G_{\text{Feed}}^{LL}$

Conclusion: L_1L_2V

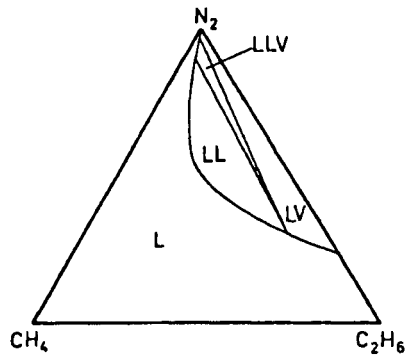

FIG. 5
The predicted phase behavior for the CH_4–C_2H_6–N_2 mixture at T = 129 K and P = 33.44 bar

Case ***A*** represents a situation when, as a result of the rigorous stability analysis applied, a zero(s) of $\Phi(y)$ with a "liquid" identification only is found. Thus a single flash calculation is needed to identify the phase configuration of the system.

Case ***B***, as a result of the stability analysis, requires two flash calculations, a liquid–liquid and a vapor–liquid, to determine the phase configuration with the lower Gibbs energy.

Cases ***C*** and ***D*** represent situations when a third flash calculation is required before the phase configuration of the system is finally determined.

Since the paper addresses the prediction and modelling of vapor–liquid–liquid equilibrium only, the case of a liquid–liquid–liquid equilibrium has not been discussed. However, its prediction and calculation could be realized quite easily applying further the same concept to any of the four paradigms.

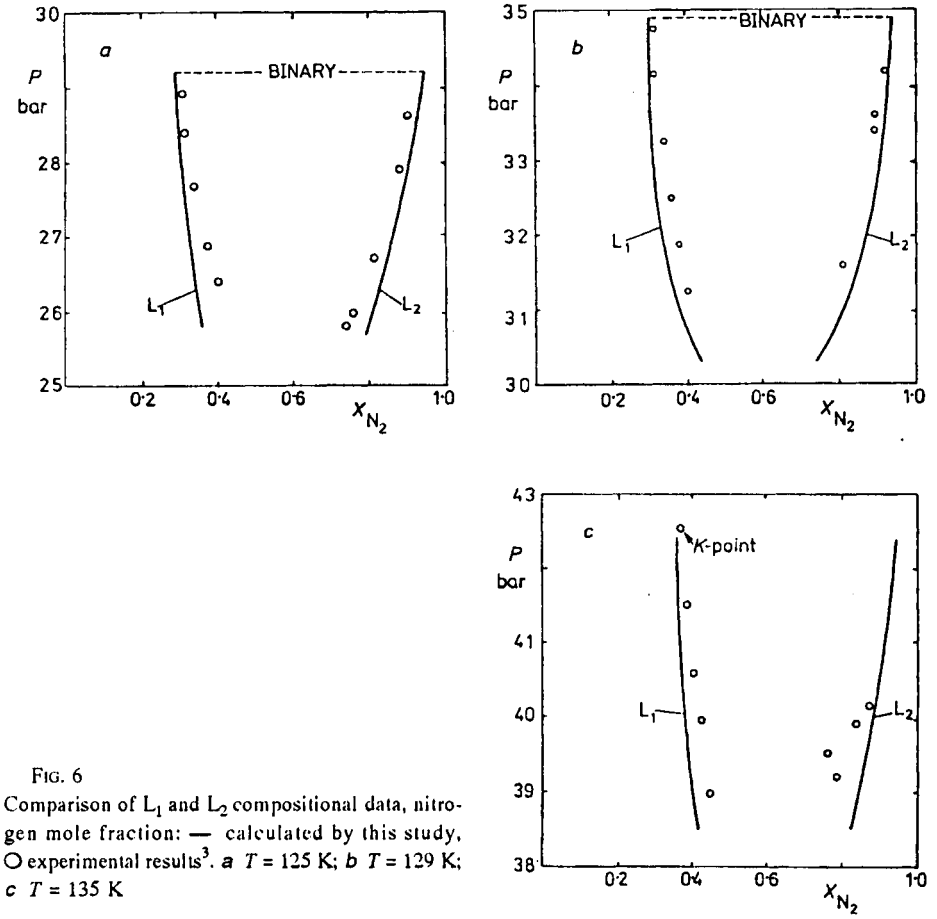

FIG. 6
Comparison of L_1 and L_2 compositional data, nitrogen mole fraction: — calculated by this study, O experimental results[3]. *a* T = 125 K; *b* T = 129 K; *c* T = 135 K

Phase Behavior Of Methane–Ethane–Nitrogen Mixture

The focus of the calculations is to describe correctly the phase behavior of the CH_4–C_2H_6–N_2 mixture, rather than to compute measured[3] phase compositions with high accuracy.

The phase configurations with the minimum Gibbs energy are determined and equilibrium compositions are calculated, applying the algorithm, outlined in the previous section of the paper, over a range of temperature from 118 K to 135 K and pressures from 18 to 42 bars.

The compositions of the L_1L_2, LV and L_1L_2V equilibrium phases, calculated at T = 118 K and P = 18.24 bar after two "liquid" and one "vapor" zeroes of $\Phi(y)$ have been found when applying the rigorous thermodynamic stability analysis, are shown in Table I. The calculations follow the paradigm, depicted as case ***D***, before the phase configuration (L_1L_2V) with minimum G is determined. The predicted phase behavior at T = 129 K and P = 33.44 bar is presented on a triangular phase diagram in Fig. 5. The calculated phase compositions for the L_1 and L_2 phases (mole fraction nitrogen) and a comparison with the measured ones[3] at the three temperatures studied in the experiment are shown in Figs 6*a* – 6*c*. The predicted curvature of the L_1L_2V region (in terms of L_1–L_2 nitrogen mole fraction data) does not differ from the experimental one. The fit of phase compositions is satisfactory. The average absolute relative deviation AARD (nitrogen mole fractions):

$$\mathrm{AARD} = \frac{1}{N}\sum_{i=1}^{N}\left|\frac{x_{N_{2_i}}^{\mathrm{calc}} - x_{N_{2_i}}^{\mathrm{exp}}}{x_{N_{2_i}}^{\mathrm{exp}}}\right|$$

is less than 3%, except in the region of the LCST, where the properties of L_1 and L_2 converge. The predicted LCST (not shown in the figures) occur at pressures that are

TABLE I

Phase calculations for the CH_4–C_2H_6–N_2 mixture at T = 118 K, P = 18.24 bar. Phase split α_{LL} = 0.10474; phase split α_{LV} = 0.06018; Gibbs energy changes: abs $[\Delta G_{\mathrm{Feed}}^{(L\text{-}V)-(L\text{-}L)}]$ = 6.09 . 10^{-5}; $\Delta G_{\mathrm{Feed}}^{(LLV)-(L\text{-}V)}$ = −6.03 . 10^{-7}

Component mole fractions							
Feed	$Liquid_1$	$Liquid_2$	Liquid	Vapor	$Liquid_1$	$Liquid_2$	Vapor
0.21	0.2154	0.1638	0.2212	0.0356	0.2213	0.1701	0.0356
0.4	0.4381	0.0746	0.4256	0.0003	0.4256	0.0777	0.0003
0.39	0.3465	0.7616	0.3532	0.9641	0.3531	0.7522	0.9641

lower than the experimental results. Since the RKS EOS binary interaction parameters were determined from LV equilibria, the poor fit in this region is not unexpected. It is possible to force a better fit by adjusting the k_{ij} through a different optimization procedure, but this is not in the scope of the present paper.

Although the calculations were not in complete quantitative agreement with measured phase compositions, the modified RKS EOS and the new computational algorithm applied did predict with reasonable accuracy the complicated phase behavior and the region of L_1L_2V, experimentally observed, of the methane–ethane–nitrogen system. Furthermore, the work has shown that for this type of mixture, consisting of non-polar components similar in size and chemical nature, the van der Waals one-fluid mixing rules with a single adjustable parameter k_{ij} are acceptable.

A future challenging task will be the correct prediction and calculation of the variety of critical end points, tricritical point and phase boundaries of the system, including the Q point locus. However, then, an introduction of a binary parameter in the combining rule for the size parameter (b) and/or a different strategy and a rigorous optimization procedure determining k_{ij}, will probably be required.

SYMBOLS

a_m	temperature dependent parameter in RKS EOS
b_m	parameter in RKS EOS
G	molar Gibbs energy
g	molar Gibbs energy hypersurface
$k_i(y)$	function of the chemical potential defference, Eq. (5)
k_{ij}	binary interaction parameter, RKS EOS
N	number of points
N_C	number of components
T	temperature
y^*	zero of the functional $\Phi(y)$ for the phase investigated
x_i	mole fraction, component i
z_i	mole fraction feed, component i
α	parameter of the RKS EOS, Eq. (1)
α,β	phase split
Φ	functional, Eq. (5)
ϕ	fugacity coefficient, component i

Superscripts

calc	calculated by the model
exp	measured by the experiment
L–L	liquid–liquid equilibrium
L–V	liquid–vapor equilibrium
L–L–V	liquid–liquid–vapor equilibrium
s	stationary
T	temperature dependent

Subscripts

Feed	referring to the system under consideration
r	reduced property
L	liquid
V	vapor

REFERENCES

1. Luks K. D., Merrill R. C., Kohn J. P.: Fluid Phase Equilib. *14*, 193 (1983).
2. Luks K. D., Kohn J. P.: *Proceedings of the 63rd Annual GPA Convention, March 19 – 21, New Orleans, Louisiana 1984.*
3. Llave F. M., Luks K. D., Kohn J. P.: J. Chem. Eng. Data *32*, 14 (1987).
4. Stryjek R., Vera J. H.: Can. J. Chem. Eng. *64*, 323 (1986).
5. Stryjek R., Vera J. H. in: *ACS Symp. Series, Equations of State – Theories and Applications* (K. C. Chao and L. R. Robinson, Eds), *300*, 560 (1986).
6. Stryjek R.: Pure Appl. Chem. *61*, 1419 (1989).
7. Stateva R. P., Tsvetkov S. G.: Technol. Today *4*, 233 (1991).
8. Fletcher R.: *Practical Methods for Optimization*, 2nd ed. Wiley, New York 1987.
9. Soave G.: Chem. Eng. Sci. *27*, 1197 (1978).
10. Michelsen M. L.: Fluid Phase Equilib. *9*, 1 (1982).
11. Michelsen M. L.: Ind. Eng. Chem. Proc. Des. Dev. *25*, 184 (1986).
12. Baker L. E., Pierce A. C., Luks K. D.: Soc. Pet. Eng. *22*, 731 (1982).